

**Master Advanced Lab Course  
Universität Göttingen – Fakultät für Physik**

---

**Report on  
the experiment KT.WZE**

**W/Z experiment at the Tevatron**

Name: Eric Bertok  
Email: eric.bertok@stud.uni-goettingen.de  
Conducted on 24th January 2018  
Assistant: Dr. J. Veatch  
Copy of document requested:  yes  no  
Unterschrift:

**Submission**

Date: Signature of assistant:

**Review**

Date: Name of examiner:  
Points: Signature:  
Mark:



## Contents

<b>1. Introduction</b>	<b>1</b>
<b>2. Theory</b>	<b>1</b>
2.1. Electroweak interaction . . . . .	1
2.2. Matrix elements and Decay rates . . . . .	1
2.3. Invariant and transverse mass . . . . .	2
<b>3. Experimental setup and methods</b>	<b>2</b>
<b>4. Analysis</b>	<b>3</b>
4.1. Selection of $Z \rightarrow \mu\mu$ events . . . . .	3
4.2. Cosmics . . . . .	4
4.3. Zmass . . . . .	4
4.4. Reconstructing and selecting $W$ events . . . . .	4
4.5. Determination of efficiencies . . . . .	9
4.6. Determination of the $BR(W \rightarrow \mu\nu)$ . . . . .	11
<b>5. Discussion</b>	<b>11</b>
<b>A. <math>Z</math> boson additional plots</b>	<b>13</b>

## 1. Introduction

The goal of this experiment is the determination the of the branching ratio of the  $W$  boson  $\text{BR}(W \rightarrow \mu\nu)$ . First,  $W$  and  $Z$  bosons are reconstructed using data provided by the Tevatron collider at Fermilab. By comparing with monte-carlo simulations, selection parameters are obtained, which allow for clean cuts for filtering out background events (jets and cosmic source). The mass and the transverse mass is then determined for the  $Z$  and  $W$  boson respectively. Finally the branching ratio is calculated from the number of selected events, the trigger efficiencies, as well as the reconstruction efficiencies.

## 2. Theory

### 2.1. Electroweak interaction

The GWS theory (Glashow, Weinberg, Salam) is the unified description of both the electromagnetic force mediated by the photon and the weak interaction mediated by the massive  $W^+$ ,  $W^-$  and the neutral neutral  $Z$  boson. It was confirmed experimentally in the 1970s [8]. The gauge bosons are introduced by means of a local  $SU(2)_L$  gauge symmetry in a weak isospin space. The weak isospin doublets are formed by fermions differing by one unit of charge [9, p.;416]. By also replacing the  $U(1)$  symmetry by a new  $U(1)_Y$  symmetry with the “hypercharge”  $Y$ , the neutral  $Z$  boson can be identified by a linear combination of the neutral  $W^{(3)}$  boson and the  $B$  boson coupling to the hypercharge. More details can be found in [9, p. 418ff]. Being a charged boson, the  $W$  bosons couple to fermions differing by one unit of charge. Furthermore it maximally violates parity as it only couples to left-handed particles and right-handed antiparticles. The vertex factor is given by [9, p.;409]

$$-i\frac{g_W}{\sqrt{2}}\frac{1}{2}\gamma^\mu(1-\gamma^5), \quad (2.1)$$

where  $g_W$  is the weak coupling constant and  $\gamma^\mu$  are the gamma matrices. The  $Z$  boson however, couples to any pair of identical fermions, albeit coupling more strongly to left handed ones. This becomes apparent in the form of the vertex factor: [9, p. 432]

$$-i\frac{1}{2}g_Z\gamma^\mu(c_V - c_A\gamma^5), \quad (2.2)$$

with the vector and axial vector couplings  $c_V$  and  $c_A$ .

### 2.2. Matrix elements and Decay rates

The matrix elements for the electroweak interaction can be calculated with the appropriate Feynman rules. After averaging over the three possible polarizations, the spin-averaged matrix element squared is obtained for both the  $W$  and the  $Z$  boson decaying to a lepton and its neutrino or a lepton- anti-lepton pair, respectively [9, p.;242,411]:

$$\langle|\mathcal{M}_W^2|\rangle = \frac{1}{3}g_W^2m_W^2 \quad (2.3)$$

$$\langle|\mathcal{M}_Z^2|\rangle = \frac{1}{3}(c_V^2 + c_A^2)g_Z^2m_Z^2. \quad (2.4)$$

These can be inserted into the decay rate formula: [9, p. 411]

$$\Gamma = \frac{p^*}{32\pi^2m^2} \int \langle|\mathcal{M}^2|\rangle d\Omega = \frac{p^*}{8\pi m^2} \langle|\mathcal{M}^2|\rangle, \quad (2.5)$$

where  $m$  is the mass of the boson and  $p^*$  is the momentum of the lepton in the center of mass frame. One can argue that  $p^* = m_Z/2$ , as the decay happens in the centre of mass frame of the decaying particle. Therefore the decay rate is

$$\Gamma(W^- \rightarrow e^-\bar{\nu}_e) = \frac{g_W^2m_W}{48\pi}. \quad (2.6)$$

$$\Gamma(Z \rightarrow e^-e^+) = \frac{g_Z^2m_Z}{48\pi}(c_V^2 + c_A^2). \quad (2.7)$$

Lepton universality tells us that this is the same for all three leptonic channels when neglecting masses. For hadronic processes, the CKM matrix has to be considered, while excluding the top quark, as it is too massive. For the  $W$  boson, one obtains for the decay width [9]

$$\Gamma_W = (3 + 6\kappa)\Gamma(W^- \rightarrow e^-\bar{\nu}_e) \approx 9.2 \frac{g_W^2 m_W}{48\pi} = 2.1 \text{ GeV}. \quad (2.8)$$

$\kappa \approx 1.038$  is a correction factor that accounts for second order QCD processes. Similarly, for the  $Z$  boson, one obtains

$$\Gamma_Z \approx 2.5 \text{ GeV}. \quad (2.9)$$

The branching ratios for the muon channel are therefore

$$BR(W \rightarrow \mu\bar{\nu}_\mu) = 10.8\%, \quad (2.10)$$

$$BR(Z \rightarrow \mu^+\mu^-) = 3.5\%. \quad (2.11)$$

### 2.3. Invariant and transverse mass

For the  $Z$  boson one can calculate the functional form of the invariant mass peak by taking into account its finite lifetime. The cross section for a  $q\bar{q} \rightarrow \mu^+\mu^-$  event is proportional to [9]

$$\sigma \propto |\mathcal{M}|^2 \propto \left| \frac{1}{q^2 - m_Z^2 + im_Z\Gamma_Z} \right|^2 = \frac{1}{(q^2 - m_Z^2)^2 + m_Z^2\Gamma_Z^2}, \quad (2.12)$$

which is a Breit-Wigner curve.  $q$  is the invariant mass of both muons. As both can be detected in such an event, the Breit-Wigner-curve can be fitted directly to the selected data to obtain the mass of the  $Z$  boson. For the  $W$  boson, things are more complicated. Due to the  $W$  events only having one muon, the undetectable neutrino has to be reconstructed from the missing momentum. For a hadron collider such as the tevatron, the total centre of mass energy cannot be known on an event to event basis due to the composite nature of the hadrons. More specifically, the  $z$ -momentum of the interacting partons are unknown, making the invariant mass reconstruction impossible. However, one can define the transverse mass  $M_T$ , which can be calculated from the reconstructed transverse momentum of the neutrino  $\mathbf{p}_T^\nu$ . First, the missing transverse energy  $MET$  is determined as

$$MET \approx |\mathbf{p}_T^\nu| = |-\mathbf{p}_T^\mu - \mathbf{u}_T|, \quad (2.13)$$

where  $\mathbf{u}_T$  is the transverse momentum of the hadrons [9]. The transverse mass is then defined as

$$M_T = \sqrt{(MET + \mathbf{p}_T^\mu)^2 - (MET_x + p_x^\mu)^2 - (MET_y + p_y^\mu)^2}. \quad (2.14)$$

This quantity is lorentz invariant but does not peak at  $m_Z$ . However, the  $W$  mass can be read off from the position of the dropoff, as the longitudinal component of the invariant mass is then close to zero.

## 3. Experimental setup and methods

For this experiment, two types of data have been provided: The first is a subset

of real data from the DØ detector at Fermilab near Chicago. The second are two sets of simulated monte-carlo  $W$  and  $Z$  events generated by PYTHIA [4].

At the DØ detector, muons are identified both in the muon detector and the tracking system. Whereas the tracking system directly surrounds the interaction point and allows for gauging the muon's momentum and direction precisely, the outer muon detector is mostly used to match the track in the tracking system. This is possible because muons are the only particles capable of reaching the muon detector, due to a combination of their relatively long lifetime and small calorimeter energy deposition. For more details on the DØ detector see [3]. As the sheer amount of data from the collider is too much to analyse and save, both software and hardware triggers are used to decide, whether an event is worth investigating. The data that is provided is pre-filtered for at least one muon in every event that has a transverse momentum of at least 15 GeV/c. The monte-carlo data has been reconstructed, such that the events look like real data. Therefore the monte-carlo serves a benchmark for the analysis of the real data. To obtain invariant mass peaks for the  $Z$ - as well as the transverse mass peak for the  $W$  boson, the right events have to be

## 4 ANALYSIS

---

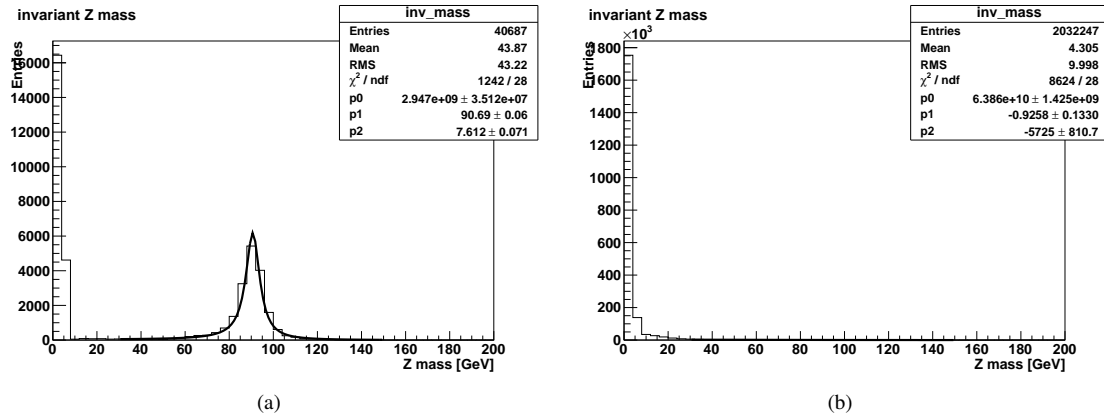


Figure 1:  $Z$  mass plotted for both monte-carlo (left) and real data (right) without any cuts. One can clearly see the expected mass peak at the monte carlo case, as well as a large number of events with very low mass, while in the real data plot, no mass peak is visible yet. For the monte-carlo case, a  $\chi^2$  fit is performed with the Breit-Wigner curve.

selected out of the 3 million events provided. This happens by first fixing a set of object level cuts, which define what is counted as a muon. These cuts are the same for both  $W$ - and  $Z$  boson analysis. Secondly, a range of object level cuts have to be performed to single out the right events for  $Z$  and  $W$  production respectively. These have to be physically motivated by keeping in mind what is expected for the muons in a  $W$  or  $Z$  decay and should also be compared to the monte-carlo simulation. By first comparing various muon parameters for the simulated data and the uncut experimental data, one can define appropriate cuts in these parameters that cut out most events not present in the simulation while also keeping events that do resemble the simulation mostly intact. Finally the real data is plotted with these cuts performed and compared with the simulated results. This process is repeated until a satisfactory isolation of  $Z$  or  $W$  events has been produced. All of the analysis is done with ROOT [5].

## 4. Analysis

### 4.1. Selection of $Z \rightarrow \mu\mu$ events

The  $Z$  boson mass distribution for the simulated monte-carlo data is shown in fig. 1(a). One can clearly see the mass peak of the  $Z$  boson. A large number of events, however, is also situated at the beginning of the mass spectrum. A fit performed by root with the function 4.1

$$\sigma \propto \frac{1}{(q^2 - m_Z^2)^2 + m_Z^2 \Gamma_Z^2} \quad (4.1)$$

is performed, with the parameters  $p_0$  as a constant proportionality factor,  $p_1$  being  $m_Z$  and  $p_2$  being the decay width  $\Gamma$ . The results are summarized together with all other fits in table 2. Apart from the large number of events at low mass, this clearly resembles the expected  $Z$  mass peak. In fig. 1(b), the uncut real data is plotted. From the 2 million events, almost all of them give a very small  $Z$  mass and the peak is not visible. Note that the trigger "TRIG\_MUW\_W\_L2M3\_TRK10" [2] is still included in the uncut case. Additional object level cuts are performed, which are summarized in table 1. These are identical for both  $Z$  and  $W$  boson analysis as they will effectively cancel out when calculating the efficiencies. The accepted and rejected events for both  $Z$  monte-carlo and real data are shown in section A (figs. 8 to 10). To further separate background events, event level cuts are performed. Firstly, events where only one muon are detected are rejected, as in a  $Z$  decay, two muons are expected. Secondly, both muons should have different charge due to conservation of charge. Two muons with same charge indicate either two separate processes both creating a positively / negatively charged muon or a cosmic event in which one cosmic muon crosses both detectors.

parameter	condition	description
$p_{T_1}$	$> 20$	transverse momentum of the first muon in the central tracker
$p_{T_2}$	$> 15$	transverse momentum of the second muon in the central tracker
$\chi^2_{1/2}$	$< 2$	Chi squared per d.o.f. for the track fit
$E_{\text{halo}_{1/2}}$	$< 1.5$	transverse calorimeter energy in an annulus of $0.1 < R < 0.4$ around the muon

Table 1: Additional object level cuts for the muons for both  $Z$  and  $W$  analysis.

Data set	$m_Z$ [GeV]	$\Gamma_Z$ [GeV]
$Z$ monte-carlo uncut	$90.69 \pm 0.06$	$7.612 \pm 0.071$
$Z$ monte-carlo cut	$91.64 \pm 0.03$	$4.448 \pm 0.088$
real data cut	$90.19 \pm 0.15$	$11.85 \pm 0.20$
Theoretical result [1]	$91.1876 \pm 0.0021$	$2.4952 \pm 0.0023$

Table 2: Summary of reconstructed  $Z$  mass  $m_Z$  and decay width  $\Gamma_Z$  for both cut and uncut simulated data ,as well as real data obtained from the Breit-Wigner fit.

## 4.2. Cosmics

The cosmic-ray background stems from high energy cosmic particles entering the earth's atmosphere, where they decay into jets of particles. Muons are also created this way. Because of time dilation, they can reach the earth's surface before they decay, leading to the cosmic background in the detector. In order to identify cosmic events, both timing and angular separation are taken into account. First, it is expected that timing differences from muons originating from  $Z$  decays have a negligible time difference at both muon detectors, since the  $Z$  boson can be treated as stationary in the lab frame. Cosmic muons, however, should be detected at one side of the detector first and at a later time on the other side, since they need to travel the distance of the detector first. The timing difference for  $Z$  monte-carlo and real data is plotted in fig. 2. A maximal time difference of  $\Delta t = 10$  ns was chosen as cut condition. However, also the simulated data shows two peaks at around 100 ns. Next, a two-dimensional histogram is plotted with the angular separation  $\Delta\eta$  and  $\Delta\phi$  as parameters.  $\eta$  is the pseudorapidity of the track and gives a measure of the tilt from the beam axis, while  $\phi$  is the angle around the beam axis. The result is shown for the simulation and real data in fig. 3. Note that so far, no angular cuts have been performed at all. Still, with the cuts given above, there is a clear preference for  $\Delta\phi = \pi$  for both simulation and real data. This is desired, as this means that the  $Z$  boson upon its decay is quasi-stationary and therefore both muons produced in the decay travel in opposite directions, as expected from momentum conservation. Therefore, a decision was made not to perform any more cuts containing angular information. As will be seen below, the cuts performed thus-far give a very satisfactory result for the reconstructed  $Z$  mass peak. The reason for this will be discussed in section 5.

## 4.3. Zmass

The invariant  $Z$  mass can be calculated directly with ROOT with the TLorentz-vector class. In theory, the muon mass is not needed for a reconstruction of the  $Z$  events, as  $E \approx p$  holds for the ultrarelativistic case, which is fulfilled for the muons in question. Finally, with the cuts performed, the  $Z$  mass is plotted in figs. 4(a) and 4(b) for both  $Z$  monte-carlo and real data. One now clearly observes the expected mass peak also in the real data. The rejected events mostly consist of low- $Z$ -mass events and cut out very little from the actual mass peak, which is especially apparent in the simulated data. Again, a fit is performed for the Breit-Wigner curve eq. (4.1). The results are summarized in table 2.

## 4.4. Reconstructing and selecting $W$ events

As outlined in section 2, the invariant  $W$  mass cannot be directly reconstructed. This is due to the neutrino in the decay products, which is not directly detectable. More specifically, the longitudinal momentum component of the  $W$  is outside of reach because of the composite structure of the colliding protons. As a result, the total centre of mass energy is unknown on an event by event basis. As the missing neutrino momentum can only be inferred from the missing energy, this means that the z-component of the energy is not detectable. It is therefore the goal to define selections that reconstruct the transverse mass eq. (2.14). The uncut transverse mass of the  $W$  monte-carlo simulation is shown in fig. 5(a). As expected, it does not peak at the  $W$  mass, however the location of the dropoff

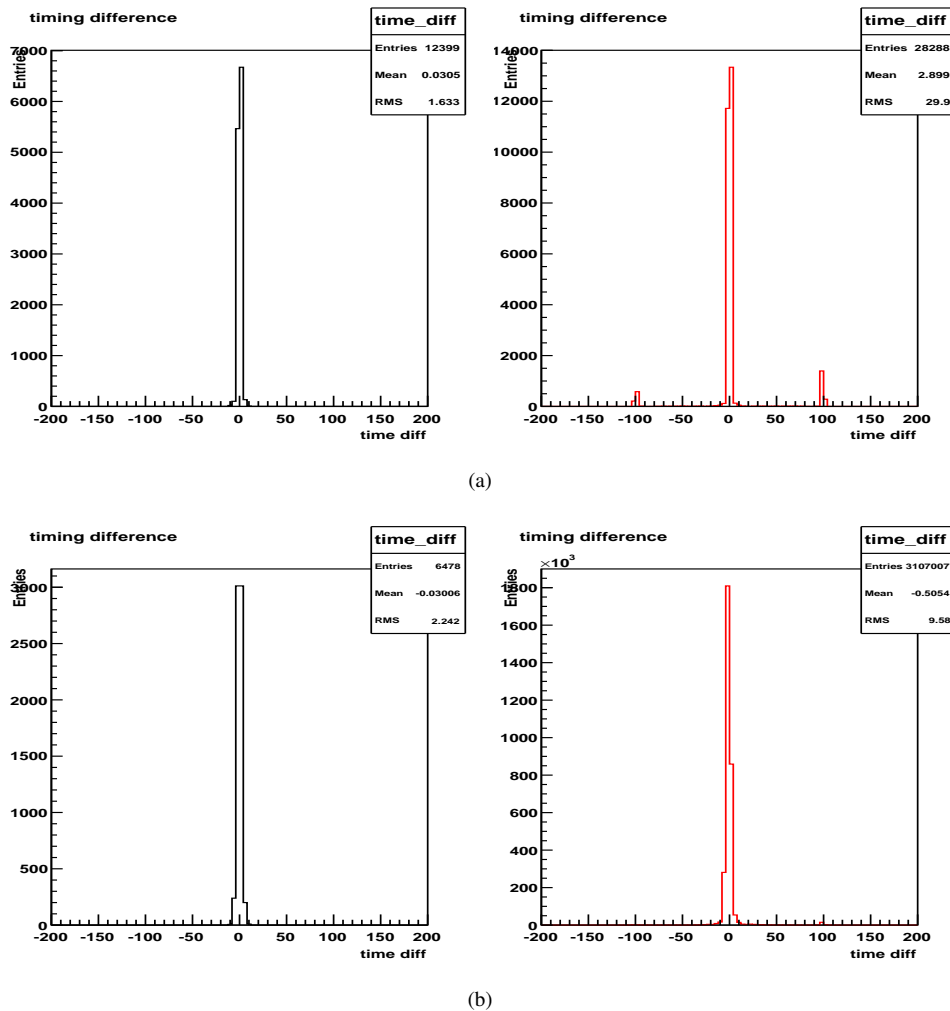


Figure 2: Timing difference between the first and second muon detection for the  $Z$  monte-carlo (a) and the real data (b) in ns. On the right: rejected events. On the left: accepted events.

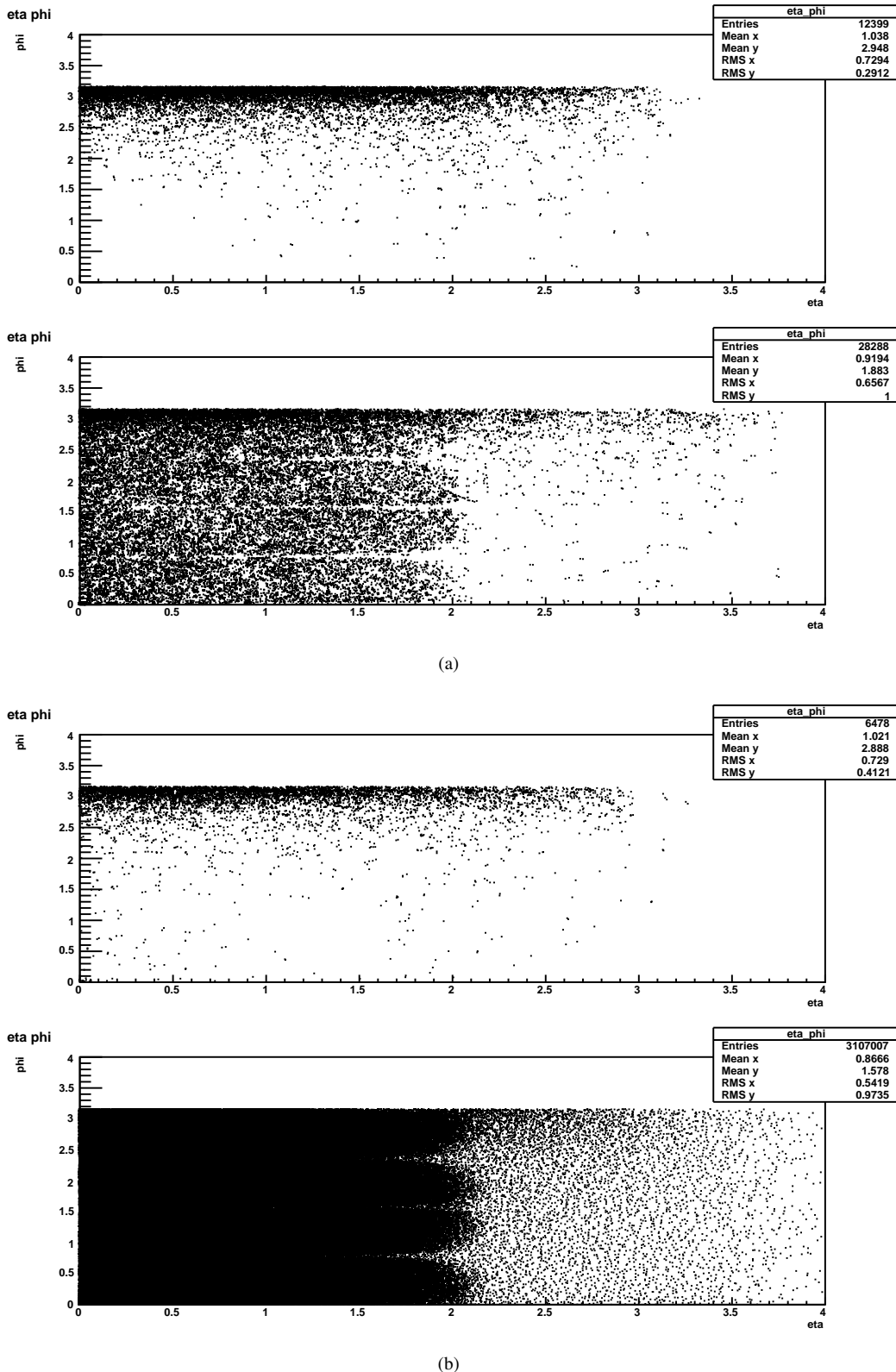


Figure 3: Two-dimensional histogram of the difference between pseudorapidity  $\Delta\eta$  and difference between azimuthal angle  $\Delta\phi$  of both muons for simulated (a) and real data (b). The upper plots are the accepted events, the lower plots are the rejected events. With the cuts detailed above, there is a clear preference of  $\Delta\phi = \pi$  in both simulation and real data. Also, lower pseudorapidity difference  $\Delta\eta$  is more common. For the uncut case, both simulation and real data shows additional structure at non- $2\pi$  azimuthal difference. Note that no angular cuts have been performed in either case.

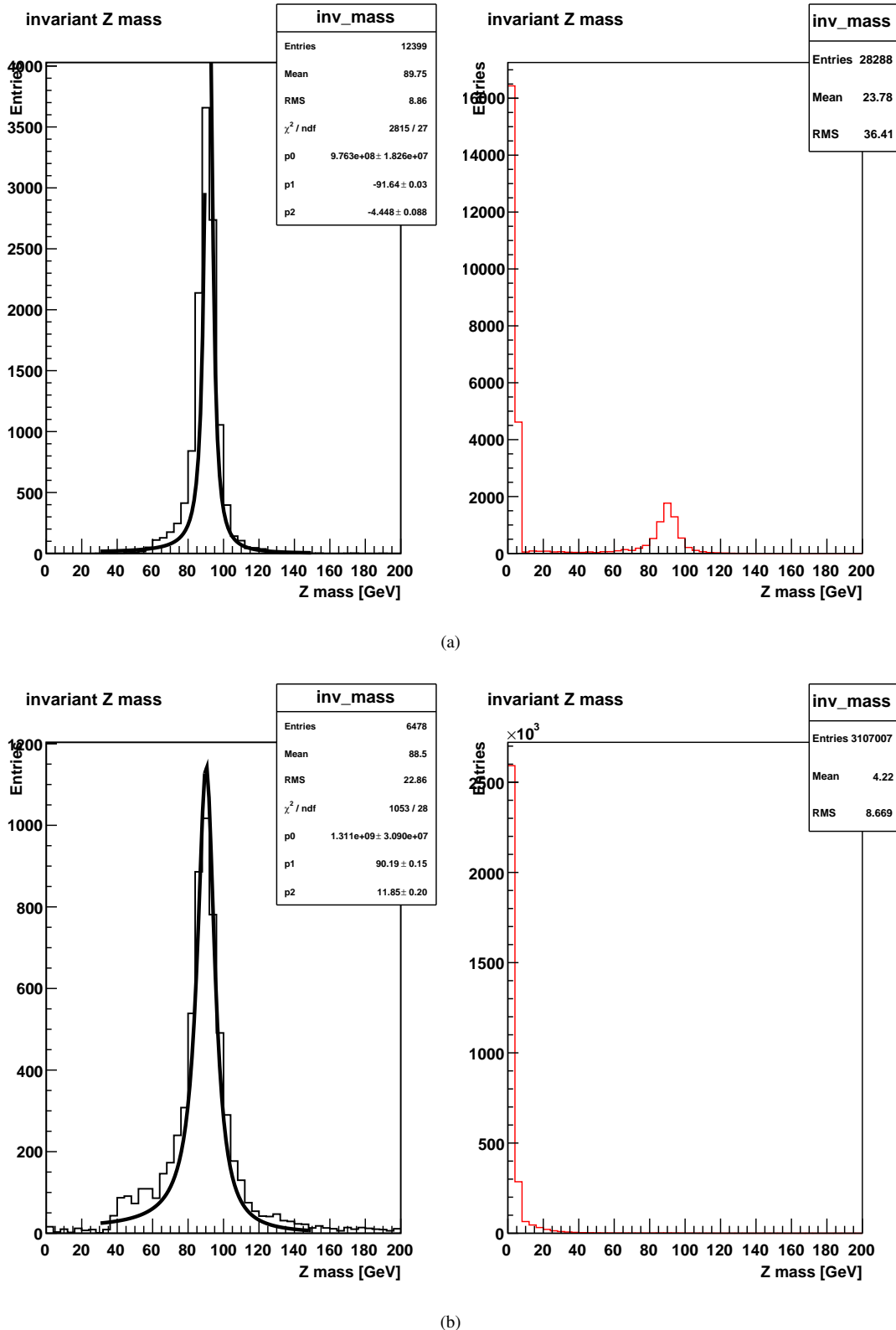


Figure 4: Reconstructed  $Z$  mass for the simulated (a) and real data (b). On the left in black, the accepted events are plotted, on the right the rejected ones. Apart from a small trail on the higher mass spectrum, both peaks look qualitatively the same. The cuts mostly got rid of the low  $Z$ -mass events, as can be seen by comparison of simulation and data. A  $\chi^2$  fit for the Breit-Wigner curve is performed on the accepted events.

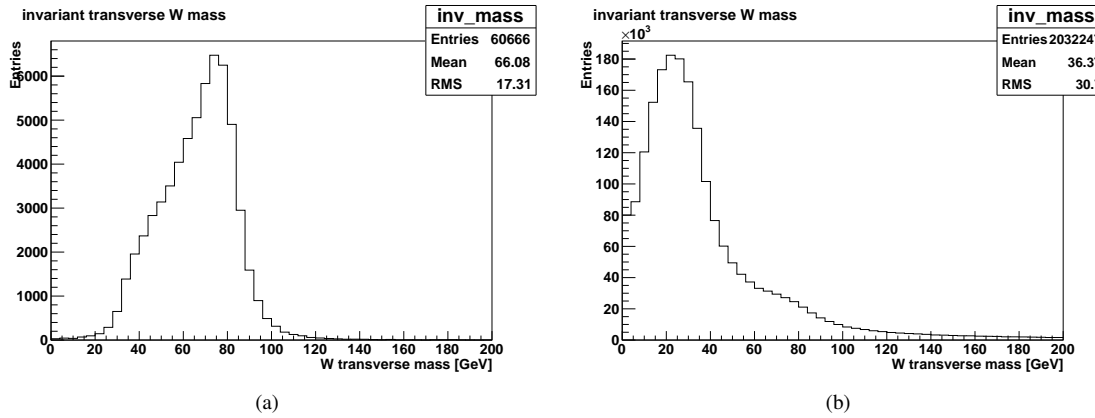


Figure 5: (a): Uncut transverse mass distribution of the  $W$  monte-carlo simulation. The dropoff occurs at around 80 GeV, which is consistent with the literature value. (b): Uncut transverse mass distribution of the real data. The data is dominated by low-transverse mass events.

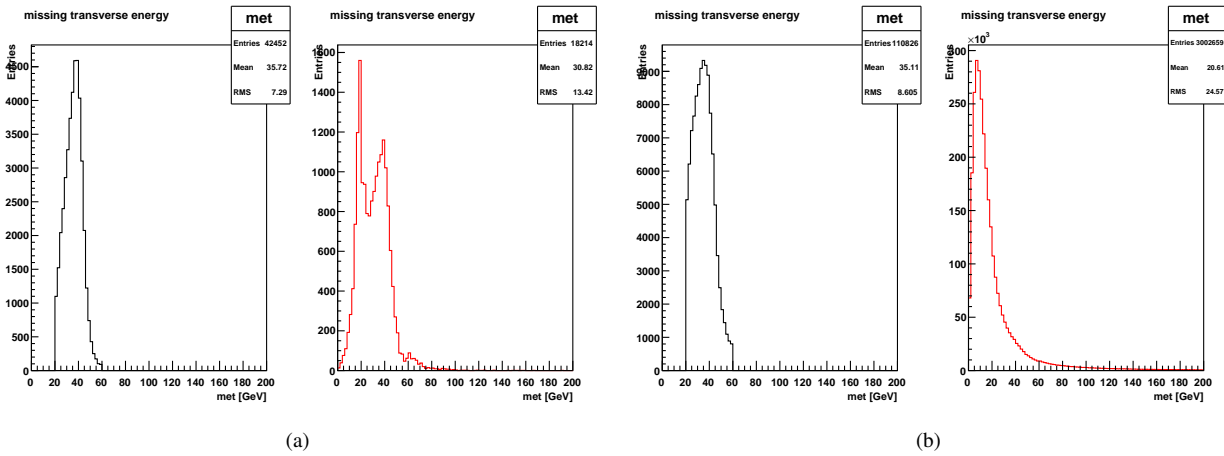


Figure 6: Missing transverse energy distribution for both simulation (a) and real data (b). Shown in black are the accepted events and in red are the rejected ones. With the cuts performed both accepted distributions look close to each other.

fits the theoretical  $W$  mass result of  $m_W = 80.385 \pm 0.015$  GeV [1]. The uncut real data plot fig. 5(b) does not have this feature: the background consisting mostly of cosmics dominates in low transverse mass regions. In addition to the object level cuts from table 1, different event level cuts are performed:

- $20 \text{ GeV} < \text{MET} < 60 \text{ GeV}$
- only one muon passes the trigger (since one muon and one neutrino is expected)

These two additional conditions are enough for a satisfactory reconstruction. Cosmics are automatically filtered out, since they almost always correspond to two muons detected at different times but only one muon is required with the selections. The condition for the missing transverse energy was mostly found by trial and error and by comparing different parameters of the simulated and the real data. The resulting MET cuts are shown in figs. 6(a) and 6(b). With the cuts in place, both accepted distributions look similar. Finally, the reconstructed transverse mass of the  $W$  boson can be calculated from eq. (2.13). It has to be kept in mind, that the muon is a minimal ionising particle and therefore does not deposit its energy into the calorimeter. Thus, when calculating the total missing transverse energy, the muon momentum has to be added which in the relativistic case is  $E_{T\mu} = p_{T\mu}$ .

The resulting transverse energy is plotted in fig. 7(b). With cuts in place, the experimental data now also shows the expected dropoff at around 80 GeV. Only around one percent of experimental events passed the selection criteria.

Mostly low  $m_T$  background was rejected. Still, also about one third of monte-carlo events were rejected, which might indicate an overselection.

## 4.5. Determination of efficiencies

In order to calculate the branching ration in section 4.6, one first has to calculate both the trigger- and the reconstruction efficiencies. The trigger efficiency is needed, since not every muon event will trigger within the detector. The ones that are missed have to be accounted for. The trigger efficiency is calculated by the independent trigger method: First, the number of events  $N_{\text{indep}}$  are counted that pass the independant trigger  $TRIG_{\text{Independant}}$ , as well as all object level cuts. The independent trigger is only determined by certain calorimeter conditions and therefore unhinged from the muon detection. Next, all events  $N_{\text{trig}}$  that additionally pass the MUW\_W\_L2M3\_TRK10 trigger used in the analysis prior is calculated. The ratio

$$\epsilon_{\text{trig}} = \frac{N_{\text{trig}}}{N_{\text{indep}}} \quad (4.2)$$

is called the trigger efficiency. One obtains

$$\epsilon_{\text{trig}} = 0.623. \quad (4.3)$$

The question now, is how to gauge the error for this efficiency. One way is to calculate the standard deviation of a binomial distribution

$$P(k|n, \epsilon_{\text{trig}}) = \frac{n!}{k!(n-k)!} \epsilon^k (1-\epsilon)^{n-k}. \quad (4.4)$$

This seems appropriate, since the probability that the special trigger is passed for a single event out of the number of all independent events  $n$  is independent from all other events and also identically distributed. Therefore, we have a sum of independent, identically distributed random variables, which gives the probability that  $k$  out of  $n$  independent events pass the trigger. The variance for the number of passed events  $k$  is now  $V(k) = n\epsilon(1-\epsilon)$  [7], from which follows via error propagation

$$V(\epsilon) = V(k/n) = \frac{V(k)}{n^2} = \frac{\epsilon(1-\epsilon)}{n}. \quad (4.5)$$

The potential problem with this treatment is that the trigger efficiency  $\epsilon$  is what is calculated and not given. Therefore, the error depends on the measurement of  $\epsilon$ . A more correct approach would be to use bayes-theorem and calculate the probability that  $\epsilon$  is the real efficiency, based on the measurements of  $k$  and  $n$ . More detail can be found in [7]. Here, we assume that the binomial approach works, especially since the biggest uncertainty comes from the reconstruction efficiencies. We thus have for the uncertainty

$$\sigma_{\epsilon_{\text{trig}}} = \sqrt{V(\epsilon_{\text{trig}})} = \sqrt{\frac{\epsilon_{\text{trig}}(1-\epsilon_{\text{trig}})}{n}}. \quad (4.6)$$

Unfortunately it was forgotten to calculate the number of events that pass the independent trigger  $n$ . In the uncut case we had around 3 million events. Even with the very strict guess that only  $n = 50000$  events were to pass the independent trigger, this would mean an uncertainty of  $\sigma_{\epsilon_{\text{trig}}} = 0.002$ , which is a reasonable value considering that the errors for the reconstruction uncertainties can only be guessed as well. For the  $Z$  boson, the trigger efficiency has to be slightly modified, since there are two seperate muons that can be detected:

$$\epsilon_{\text{trig},Z} = \epsilon_{\text{trig}}^2 + \epsilon_{\text{trig}}(1-\epsilon_{\text{trig}}) + (1-\epsilon_{\text{trig}})\epsilon_{\text{trig}} = -\epsilon_{\text{trig}}^2 + 2\epsilon_{\text{trig}}, \quad (4.7)$$

which is the sum of the probabilities that both muons trigger and the probability that exactly one muon triggers.

Next, the reconstruction efficiencies are determined, which for both bosons are defined by

$$\epsilon_{\text{rec}} = \frac{\# \text{ of reconstructed events in monte-carlo}}{\# \text{ total events in monte-carlo}}. \quad (4.8)$$

The results are

$$\epsilon_{\text{rec},W} = \frac{42452}{60666} = 0.700, \quad \epsilon_{\text{rec},Z} = \frac{12399}{40687} = 0.305. \quad (4.9)$$

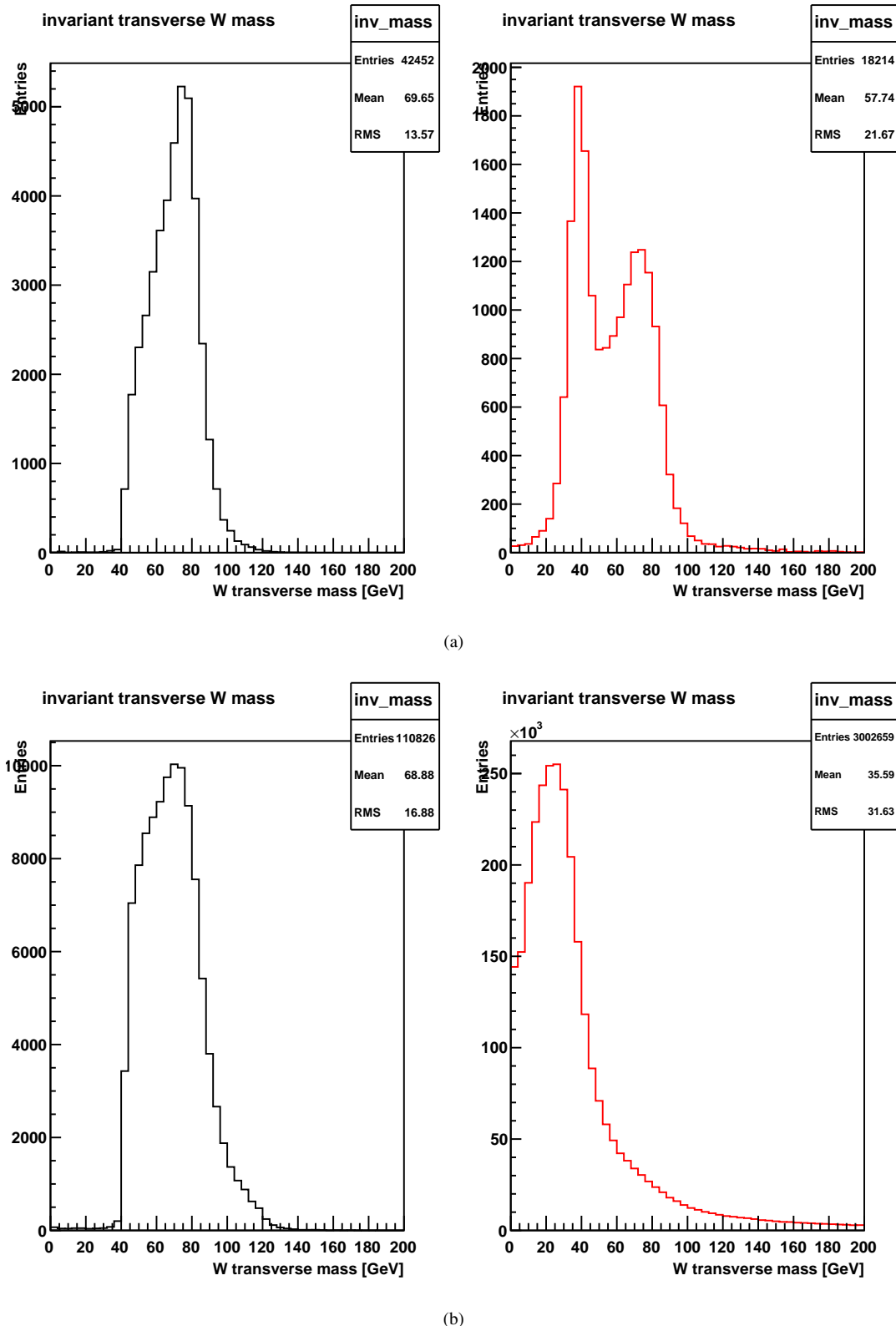


Figure 7: Reconstructed transverse  $W$  mass for the simulated data with cuts (a) and for the cut real data (b). In black: selected events. In red: rejected events. The selection mostly rejected low  $m_T$  background. The expected dropoff at around 80 GeV is now visible for the experimental data. However, also about one third of monte-carlo events were rejected by our selection.

Additionaly, the misidentification rate

$$\epsilon_{\text{miss}} = \frac{\# \text{ reconstructed fake } W \text{ bosons}}{\# \text{ total } Z \text{ bosons}} = \frac{14641}{40687} = 0.360 \quad (4.10)$$

has to be taken into account. It is calculated by running the  $W$  selection algorithm over the  $Z$  monte-carlo data to find how many are misidentified. It has to be assumed that this misidentification rate as calculated solely for the simulated data reflects the real world misidentification of  $W$  bosons. This is a crude approximation. Ideally one would like to directly calculate this value from the experimental data. For this one would need to identify events where a muon is detected but none is found, which is out of scope of this report. For more details see the “tag and probe method” [6].

#### 4.6. Determination of the $BR(W \rightarrow \mu\nu)$

The theoretical cross sections are given in [2]:

- $\sigma(p\bar{p} \rightarrow W + X) = 23.7 \text{ nb}$
- $\sigma(p\bar{p} \rightarrow Z + X) = 7.18 \text{ nb}$
- $BR(Z \rightarrow \mu\mu) = 3.366 \pm 0.007\%$ .

The ratio of  $W$  and  $Z$  events is given by [2]

$$R = \frac{\sigma(p\bar{p} \rightarrow W + X)BR(W \rightarrow \mu\nu)}{\sigma(p\bar{p} \rightarrow Z + X)BR(Z \rightarrow \mu\mu)} = \frac{N_W}{N_Z}, \quad (4.11)$$

where  $N_{W/Z}$  is the total amount of real  $W/Z$  events (not just those that passed the trigger). The integrated luminosity is not needed as it cancels out. The number of reconstructed events can be written in terms of the true number contained in the data:

$$N_{\text{rec},W} = (N_W \epsilon_{\text{rec},W} + N_Z \epsilon_{\text{miss}}) \epsilon_{\text{trig},W}, \quad (4.12)$$

$$N_{\text{rec},Z} = (N_W \epsilon_{\text{rec},Z}) \epsilon_{\text{trig},Z} \quad (4.13)$$

Rearranging the terms from eqs. (4.11) and (4.12) one finally obtains

$$BR(W \rightarrow \mu\nu) = \left( \frac{N_{\text{rec},W} \epsilon_{\text{rec},Z} \epsilon_{\text{trig},Z}}{N_{\text{rec},W} \epsilon_{\text{rec},Z} \epsilon_{\text{trig},Z}} - \frac{\epsilon_{\text{miss}}}{\epsilon_{\text{rec},W}} \right) \frac{\sigma(p\bar{p} \rightarrow Z + X)BR(W \rightarrow \mu\mu)}{\sigma(p\bar{p} \rightarrow W + X)} = 9.95\%. \quad (4.14)$$

## 5. Discussion

First, it has to be pointed out that overall very few event level cuts have been used. Almost all cuts have been object level  $p_T$ ,  $\chi^2$  and  $E_{\text{halo}}$  cuts, which are identical for both  $Z$  and  $W$  analysis. The only event level cuts used were the charge of the muon(s) and their number. It seems surprising that the  $Z$  mass could still be reconstructed successfully, as can be seen in table 2. Neither of the values are within their one sigma confidence intervals that the fit gave us, however both the uncut monte-carlo, as well as the cut monte-carlo and the measured value with the real data is very close to the literature value with a maximal relative difference of 1% with the real data value. Both monte-carlo results have the same relative difference of 0.5% and are therefore slightly more accurate. The theoretical decay width is almost one order of magnitude lower than the measured value. This can be explained by the fact that the reconstructed, not the actual  $Z$  mass peak was measured. Spectral broadening inside of the detector tends to widen the variance of the data.

The reconstructed  $Z$ -mass plot fig. 4(b) shows a qualitatively very good reconstruction of the peak. It can also be seen that the selection conditions mostly eliminated low  $m_T$  background. As our analysis suggests this background consists mostly of cosmics: A muon going through both sides of the detector gives effectively the muon’s rest mass as invariant mass. The fact that the selection conditions were enough probably rests on the charge cuts that instantly filter out the cosmic events (that all have the same charge) without needing to further analyse the angular distributions. But there is also the risk of overcutting: On the one hand, around two thirds of the monte-carlo data has been cut out by our selections. On the other hand, most of the rejected data consists of the background as evident in fig. 4(a).

For the  $W$  boson, only the MET cuts as well as the forced number and charge of muons have been utilised. Qualitatively the reconstructed  $W$  transverse mass distribution looks very promising. A detailed determination of the  $W$  mass was not done however, and might make the result less optimal. Hints for this are seen in the  $W$  monte-carlo plots figs. 7(a) and 7(b): The selection rejected around one third of the  $W$  monte-carlo events. Therefore there has probably been an overselection of events. A larger focus on event-based cuts like angular distribution should be done before doing strict object-level cuts, as we have done. Especially more 2d-histograms could have helped to find the right selections.

Another improvement can be made for the trigger efficiency, for which it was forgotten to calculate the number of events that pass the independent trigger. It is questionable whether the crude approximation of  $n = 50\,000$  events is reasonable, but it was used to create an approximate upper bound to the error, since the error only shrinks with a larger  $n$ .

The reconstruction efficiencies eq. (4.9) show, that  $W$  events are more effectively reconstructed than  $Z$  events. However, also about one third of all  $Z$  bosons are misidentified as a  $W$  boson. Still, these efficiencies were calculated with the simulated data only. There is no guarantee that the real data behaves in the same way to the cuts we have chosen. Finally, the branching ratio of the  $W$  boson that was measured here has a 7% relative difference to the literature value. While this has the right order of magnitude, one cannot be confident with this value, because no real error propagation could be calculated without the tag and probe method. Summing up, this lab has provided a very nice introduction into data analysis with root, as well as standard practices commonly used in particle physics. With more background knowledge one could have spent more time on finetuning the selections which in turn could have provided a better end result. Still, qualitatively one can be content with the result that was found in a few hours of data analysis.

## References

- [1] *Particle Data Group: gauge boson summary sheet.* <http://pdg.lbl.gov/2017/tables/rpp2017-sum-gauge-higgs-bosons.pdf>. – Zugriff:2018-01-31
- [2] *Praktikumshandbuch.* master-fp.physik.uni-goettingen.de. – Zugriff:2018-01-31
- [3] *Public web page of the DØ experiment.* <http://www-d0.fnal.gov/public/index.html>. – Zugriff:2018-01-31
- [4] : *Pythia homepage.* <http://home.thep.lu.se/Pythia/>
- [5] : *ROOT homepage.* <https://root.cern.ch/>
- [6] : *Tag and probe, twiki.* <https://twiki.cern.ch/twiki/bin/view/CMSPublic/TagAndProbe>
- [7] : *Treatment of Errors in Efficiency Calculations.* <http://th-www.if.uj.edu.pl/~erichter/dydaktyka/Dydaktyka2012/LAB-2012/0701199v1.pdf>
- [8] *Wikipedia: electroweak interaction.* [https://de.wikipedia.org/wiki/Elektrroschwache\\_Wechselwirkung](https://de.wikipedia.org/wiki/Elektrroschwache_Wechselwirkung). – Zugriff:2018-01-31
- [9] THOMSON, Mark: *Modern Particle Physics*. Cambridge University Press, 2013

**A. Z boson additional plots**

## A Z BOSON ADDITIONAL PLOTS

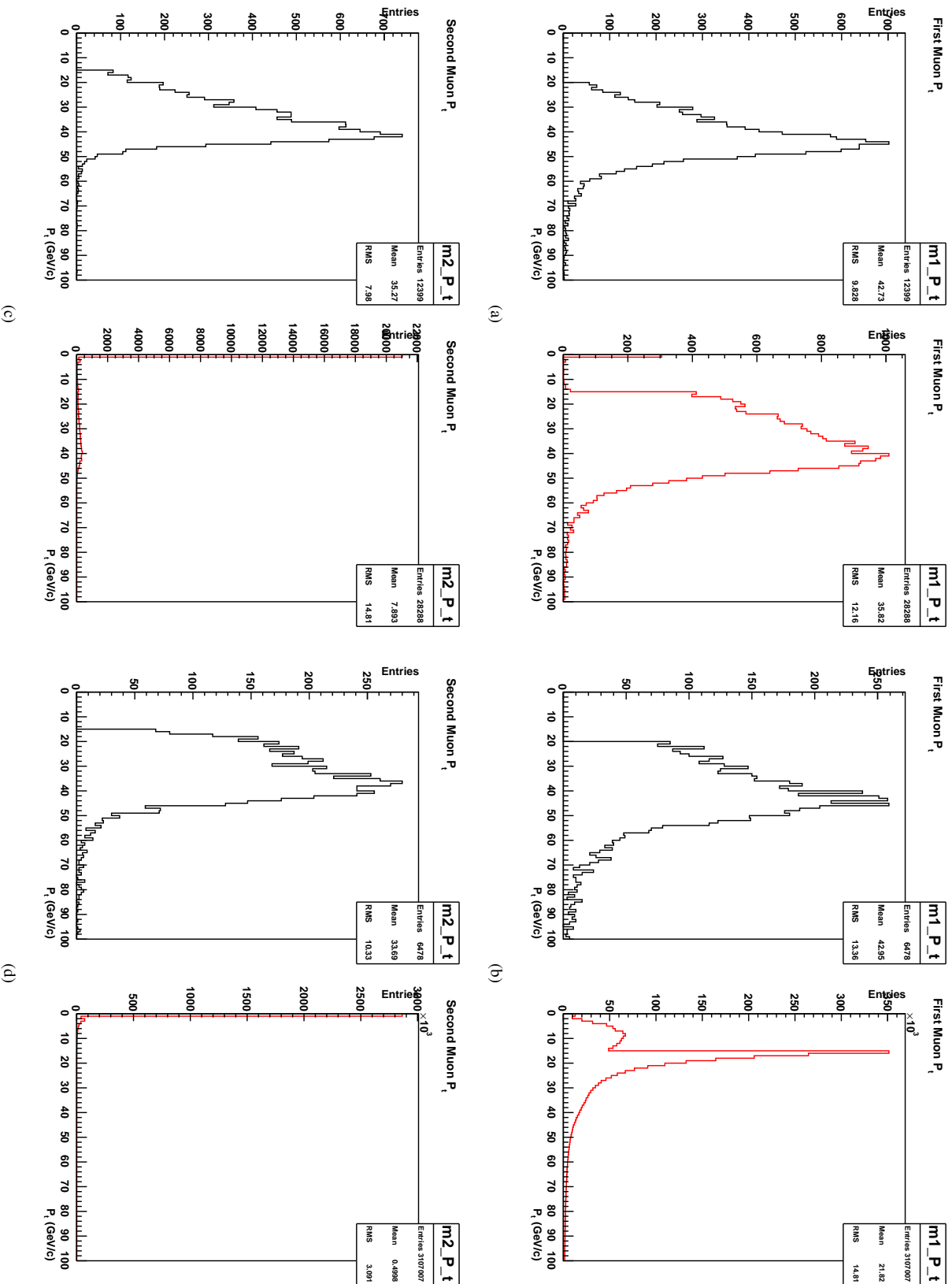


Figure 8:  $p_T$  for accepted (black) and rejected (red) events for (a,c): the  $Z$  monte-carlo data (b,d): the real data.

## A Z BOSON ADDITIONAL PLOTS

---

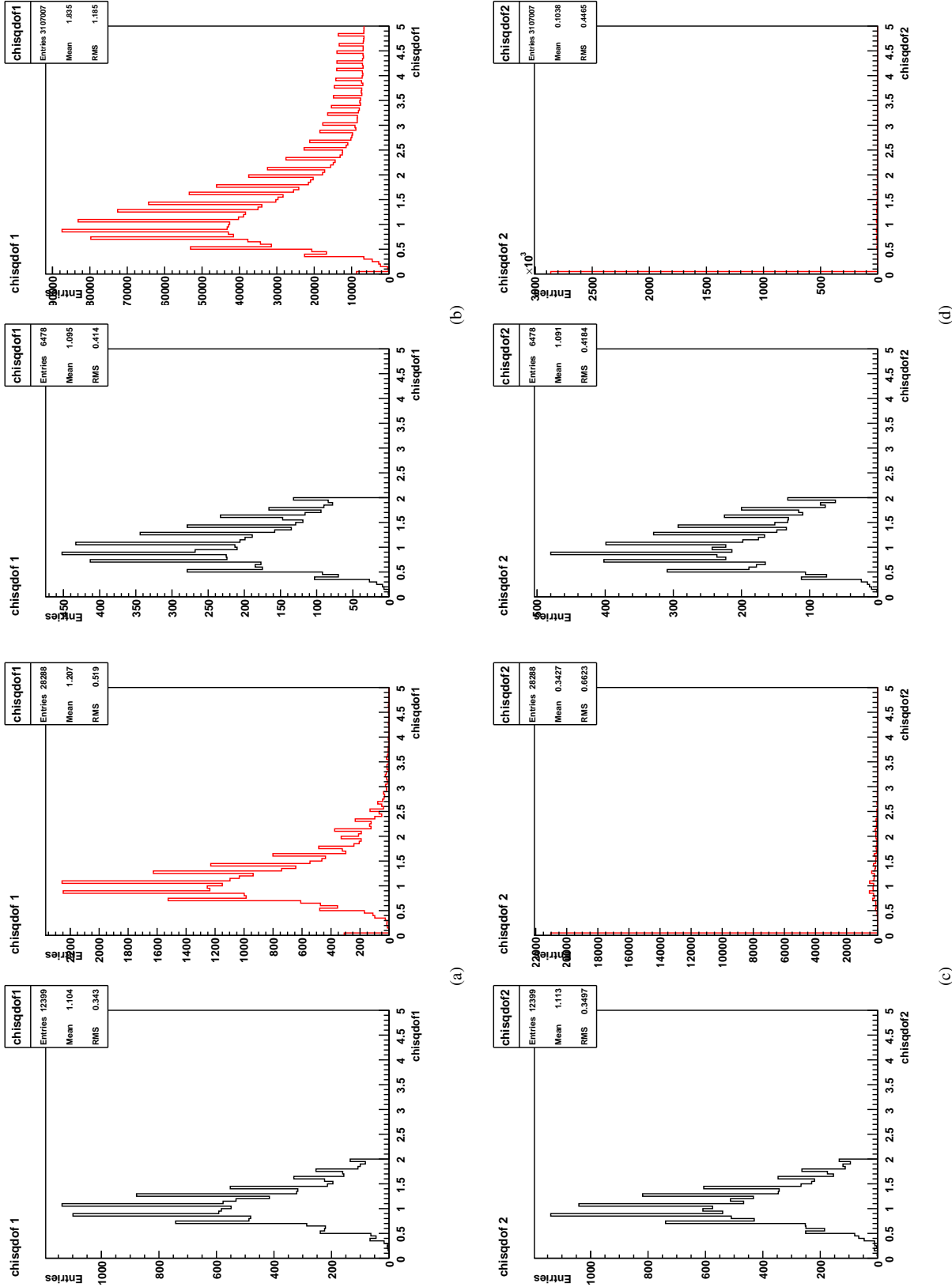


Figure 9:  $\chi^2$  for accepted (black) and rejected (red) events for (a,c): the  $Z$  monte-carlo data (b,d): the real data.

## A Z BOSON ADDITIONAL PLOTS

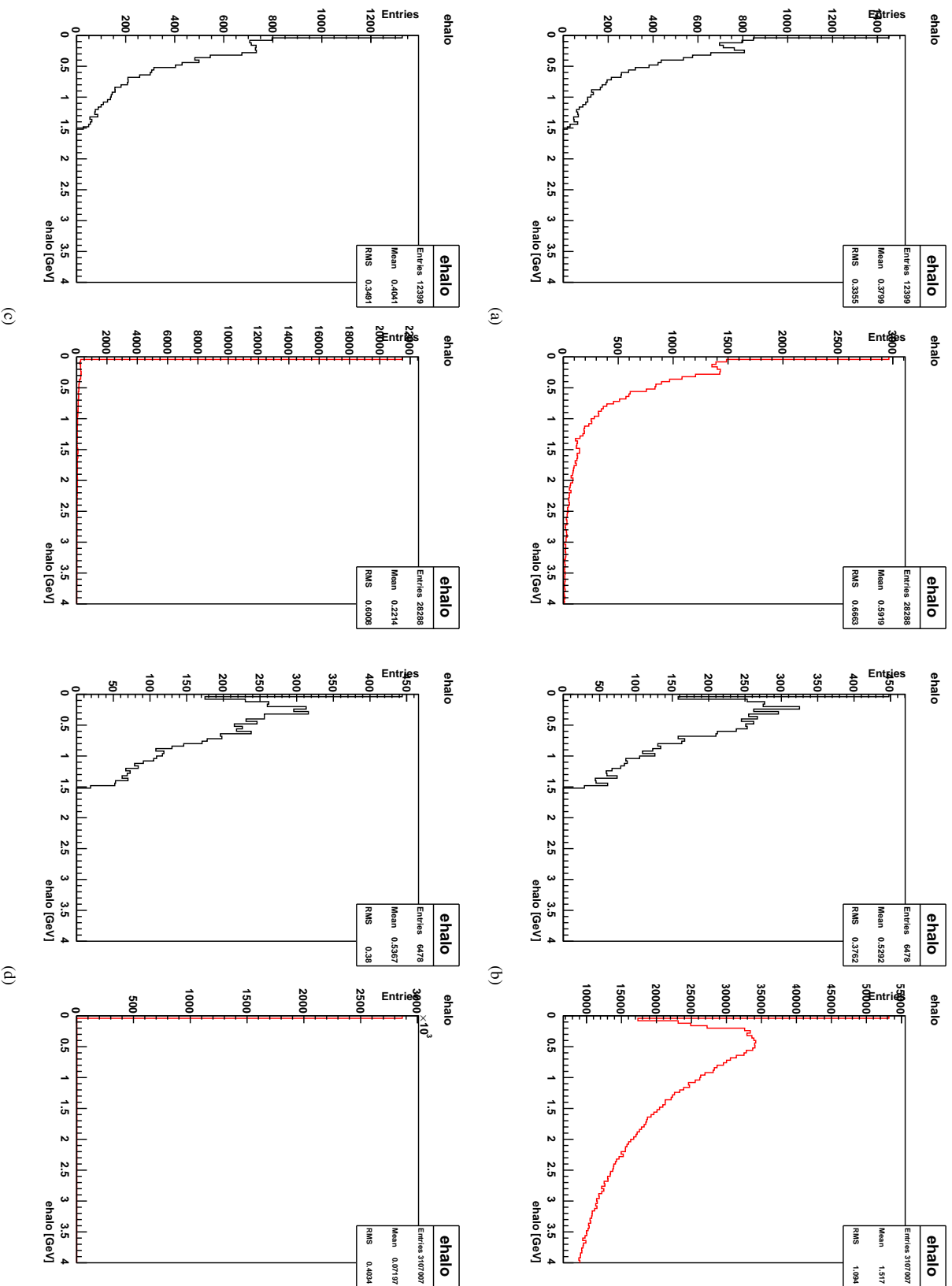


Figure 10:  $E_{\text{halo}}$  for accepted (black) and rejected (red) events for (a,c); the  $Z$  monte-carlo data (b,d); the real data.